NF1 is a critical regulator of muscle development and metabolism

Kate Sullivan[1,†], Jad El-Hoss[1,3,†], Kate G.R. Quinlan[2,3], Nikita Deo[1,3], Fleur Garton[2,3], Jane T.C. Seto[2,3], Marie Gdalevitch[1], Nigel Turner[5,6], Gregory J. Cooney[5,6], Mateusz Kolanczyk[4], Kathryn N. North[2,3], David G. Little[1,3] and Aaron Schindeler[1,3,*]

[1]Orthopaedic Research & Biotechnology Unit and [2]Institute for Neuroscience and Muscle Research, The Children's Hospital at Westmead, Sydney, Australia, [3]Discipline of Paediatrics and Child Health, Faculty of Medicine, University of Sydney, Sydney, Australia, [4]FG Development & Disease, Max Planck Institute for Molecular Genetics, Berlin, Germany, [5]Diabetes and Obesity Research Program, Garvan Institute of Medical Research, Darlinghurst, Australia and [6]UNSW Medicine, University of New South Wales, Sydney, Australia

There is emerging evidence for reduced muscle function in children with neurofibromatosis type 1 (NF1). We have examined three murine models featuring NF1 deficiency in muscle to study the effect on muscle function as well as any underlying pathophysiology. The $Nf1^{+/-}$ mouse exhibited no differences in overall weight, lean tissue mass, fiber size, muscle weakness as measured by grip strength or muscle atrophy-recovery with limb disuse, although this model lacks many other characteristic features of the human disease. Next, muscle-specific knockout mice ($Nf1_{muscle}^{-/-}$) were generated and they exhibited a failure to thrive leading to neonatal lethality. Intramyocellular lipid accumulations were observed by electron microscopy and Oil Red O staining. More mature muscle specimens lacking $Nf1$ expression taken from the limb-specific $Nf1_{Prx1}^{-/-}$ conditional knockout line showed a 10-fold increase in muscle triglyceride content. Enzyme assays revealed a significant increase in the activities of oxidative metabolism enzymes in the $Nf1_{Prx1}^{-/-}$ mice. Western analyses showed increases in the expression of fatty acid synthase and the hormone leptin, as well as decreased expression of a number of fatty acid transporters in this mouse line. These data support the hypothesis that NF1 is essential for normal muscle function and survival and are the first to suggest a direct link between NF1 and mitochondrial fatty acid metabolism.

INTRODUCTION

Neurofibromatosis type 1 (NF1) is a genetic disorder that is associated with a range of features including superficial and deep neurofibromas, developmental delay affecting both cognitive and motor performance and musculoskeletal complications (1). In recent years, the complexity of the musculoskeletal manifestations has been elaborated on by a number of basic, translational and clinical studies (2). Whereas there has been substantive progress in exploring the bony abnormalities, only recently has muscle emerged as a tissue of interest in individuals with NF1.

While scoliosis and congenital dysplasias (particularly tibial dysplasia) have long been part of the standard diagnostic criteria

for NF1, individuals with this condition are also prone to low bone mineral density (BMD) (3,4). While low BMD can correlate with orthopedic complications such as scoliosis, population studies have yet to demonstrate a significant correlation with fracture risk (5,6). These bony manifestations have now been mechanistically linked to several underlying causes. Focal bone defects such as congenital tibial dysplasia have been associated with local double inactivation of NF1, and this may be the basis for some cases of dystrophic scoliosis (7). In contrast, low BMD is more likely to result from haploinsufficiency for NF1 leading to increased osteoclast activity (8). Many additional bone dysplasias associated with NF1 (sphenoid wing dysplasia, *pectus excavatum*, rib penciling) still have an unknown etiology, but may result from deficiencies in developmental patterning.

*To whom correspondence should be addressed at: Orthopaedic Research & Biotechnology, The Children's Hospital at Westmead, Research Building, Locked Bag 4001, Westmead, NSW 2145, Australia. Tel: +61 298451451; Fax: +61 298453078; Email: aaron.schindeler@sydney.edu.au
†Both authors contributed equally to this work.

In 1994, the *NF1* gene product neurofibromin was found to be upregulated during myoblast differentiation, suggesting a potential role in muscle (9). Nevertheless, the deficits in motor skills and co-ordination associated with NF1 have been historically attributed to central nervous system dysfunction (10). Lately, however, a number of clinical reports have identified decreases in muscle size (11,12), strength (13,14) and motor proficiency (15), leading to renewed speculation regarding primary muscle involvement. Muscle weakness could also contribute to systemic osteopenia due to decreased loading, and load-carrying regions of the skeleton are reported as the most affected (3,11). Still, the interactions between muscle and bone, particularly as a modifying factor for BMD and fracture risk, remain unclear.

Recent work with the $Nf1_{Prx1}{}^{-/-}$ mouse (*Prx1-cre* driven *Nf1* deletion in the limbs) has reinforced the importance of NF1 in muscle development (12). In this study, $Nf1_{Prx1}{}^{-/-}$ mice were studied from the earliest stages of limb bud morphogenesis. These mice display a congenital myopathy characterized by reduced muscle fibers, reduced muscle force and fibrosis. Neurofibromin is a key negative regulator of Ras signaling, and can activate a variety of downstream pathways including c-Jun N-terminal kinase (JNK), phosphoinositide 3-kinase (PI3K) and mitogen-activated protein kinase (MAPK) pathways. Muscle extracts from adult $Nf1_{Prx1}{}^{-/-}$ mice showed increased MAPK signaling, but signaling intermediate cAMP was also dysregulated. Both cAMP and mitochondrial enzyme dysfunction have also been reported in *nf1*-deficient fruitflies (16). Interestingly, in the fly model, cAMP analogues were able to ameliorate the *nf1* phenotype.

While the $Nf1_{Prx1}{}^{-/-}$ mouse demonstrates a critical role for *Nf1* in limb development, *Prx1-cre* expression affects all mesenchymal lineages of the developing limbs, including adipocytes and vasculature endothelial cells (12). It also does not specifically address whether NF1 heterozygous mice manifest a muscle phenotype. Consequently, we sought to examine muscle function in a range of different NF1 mouse models.

First, we investigated muscle structure and function in the heterozygous $Nf1^{+/-}$ mouse; $Nf1^{-/-}$ knockout is embryonic lethal (17). Grip strength testing was performed and muscle tissue was examined by histology. Next, the capacity of $Nf1^{+/-}$ muscle to respond to stress was tested in a botox-induced disuse atrophy/

recovery model. To specifically examine the biological importance of the *Nf1* gene in muscle, we generated a muscle-specific double knockout of NF1 using the *MyoD-cre* and $Nf1^{flox/flox}$ lines (18,19). This $Nf1_{MyoD}{}^{-/-}$ line showed a severe muscle phenotype resulting in neonatal lethality. Lastly, some of the histological and metabolic features revealed by the $Nf1_{MyoD}{}^{-/-}$ neonates were examined in *Nf1*-null muscle tissue from mature $Nf1_{Prx1}{}^{-/-}$ mice.

RESULTS

Heterozygosity for Nf1 deficiency does not affect muscle size, fiber size or force

Prior studies have indicated that the $Nf1^{+/-}$ mice can manifest some but not all of the clinical features NF1. To examine concordance between clinical reports of human grip weakness (14), and the heterozygous mouse, grip strength of $Nf1^{+/-}$ mice was measured using a mouse grip strength meter. No difference was seen compared to wild-type (WT) littermates (Fig. 1A). No significant difference was seen in body weight with $Nf1^{+/-}$ mice, as has been previously shown ($P = 0.16$), thus specific force was also unchanged. Examination of muscle fiber size showed initially no difference, although fiber size is known to vary by fiber type. Consequently, sections from the *tibialis anterior* of $Nf1^{+/-}$ and WT mice were stained for fiber type. No significant differences in fiber size were observed (Fig. 1B).

$Nf1^{+/-}$ mice show no significant difference in recovery following muscle injury

To examine the response of $Nf1^{+/-}$ mice to limb disuse, the hind limb musculature was locally injected with Botox. Mice were analyzed for gait and weight until they were ambulating normally. Botox treatment caused a decrease in ambulation that corresponded with a decrease in body weight in both the WT and $Nf1^{+/-}$ mice (Supplementary Material, Fig. S1). There was no significant difference in the total body weight lost or the time taken to regain this weight in either group. Functionally, there was no difference in the time to restore normal gait.
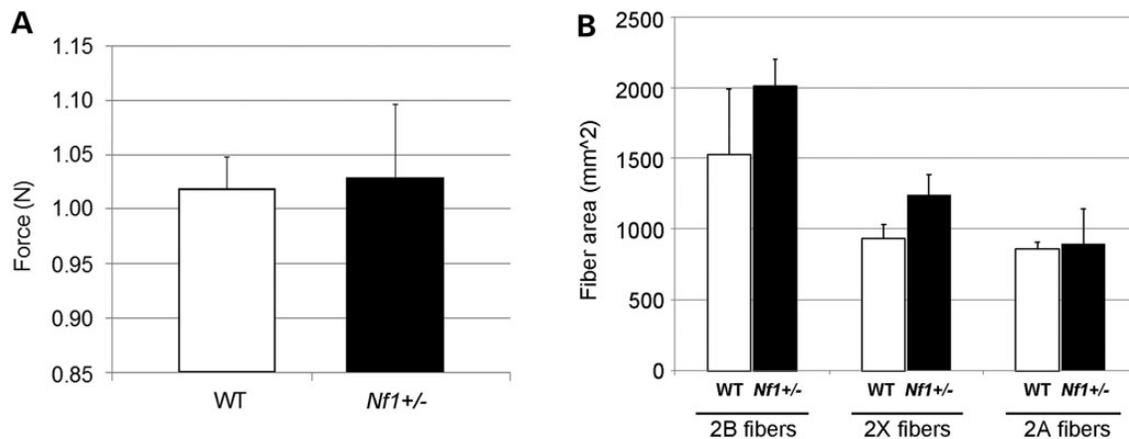

Figure 1. The $Nf1^{+/-}$ mouse line showed (**A**) no significant difference in grip strength compared with WT controls ($P = 0.83$), and (**B**) no significance in fiber size for type 2B, 2X, 2A fibers, respectively.

Lean tissue mass in the affected limb was measured by DEXA (Fig. 2). While this demonstrated rapid loss of lean tissue in the Botox-treated animals over the first 3 weeks followed by progressive recovery, no difference was seen between WT and $Nf1^{+/-}$ mice. Mice were harvested at 1, 2, 3 and 12 weeks for more detailed muscle quantification by microCT (Supplementary Material, Fig. S2A) or muscle wet weight (Supplementary Material, Fig. S2B). Botox induced muscle loss was observed, but *Nf1* deficiency did not affect muscle loss or recovery in the heterozygous mouse line.
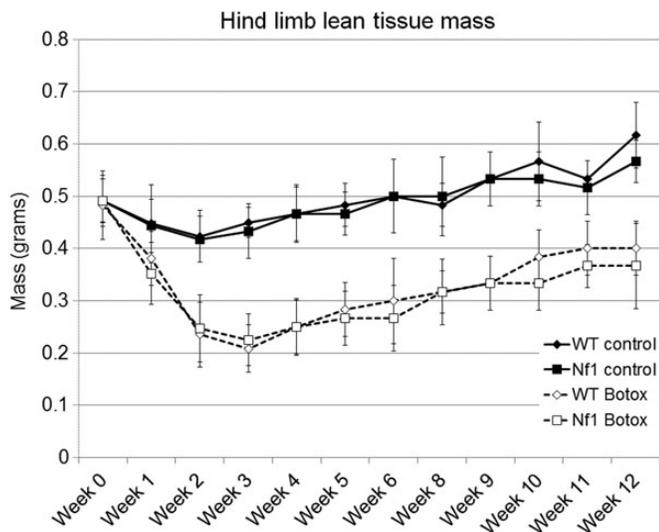

Figure 2. Analysis of loss of lean tissue mass in the Botox-treated limb in WT and $Nf1^{+/-}$ mice. Following Botox-induced limb disuse, WT and $Nf1^{+/-}$ mice underwent weekly DEXA analysis to quantify lean tissue mass. In WT and $Nf1^{+/-}$ mouse strains, Botox lead to a significant reduction in lean tissue mass (broken line) compared with untreated control (solid line). There was no difference in loss or recover of lean tissue mass in $Nf1^{+/-}$ mice compared with WT mice with Botox treatment ($P > 0.05$).

$Nf1^{+/-}$ mice show greater acute cortical bone loss with unloading

Prior analyses had shown no significant difference in bone parameters between $Nf1^{+/-}$ and WT mice, although fracture repair was delayed (20). To examine bone loss and recovery with disuse, bone mineral content and bone volume (BV) were analyzed by X-ray, DXA and microCT.

Analysis of the tibia by microCT showed rapid bone loss following botox treatment in all mice. The $Nf1^{+/-}$ mice exhibited a more rapid loss of cortical bone with unloading (Fig. 3). Loss of trabecular bone and the ability to recover both cortical and trabecular bone at 12 weeks after the resumption of load were statistically no different between $Nf1^{+/-}$ and WT mice.

Muscle-specific KO of *Nf1* causes decreased body weight and neonatal lethality

To explore the functional role of neurofibromin in muscle tissue, we generated a muscle-specific *Nf1* knockout mouse driven by *MyoD-cre*. *Nf1* gene recombination has been previously reported in muscle isolated from this line (21). Conditional knockout mice were analyzed at days 2, 4 and 6, and weighed significantly less than control litter mates (Fig. 4). While smaller, the mutant mice did not show shortened or bowed long bones or impaired mobility. Autopsy of dead $Nf1_{muscle}^{-/-}$ pups showed the presence of milk in their stomachs, evident of some capacity for suckling. No organ failure was apparent in the post-mortem. The primary cause of death was attributed to maternal infanticide, likely due to their inability to thrive compared with littermates.

Ultrastructural analysis of *Nf1* knockout muscle tissue

Ultrathin sections of muscle were analyzed from $Nf1_{muscle}^{-/-}$ mice and littermate controls by transmission electron microscopy (EM). While it was hypothesized that force generation may be compromised due to deficiencies in cytoarchitecture,
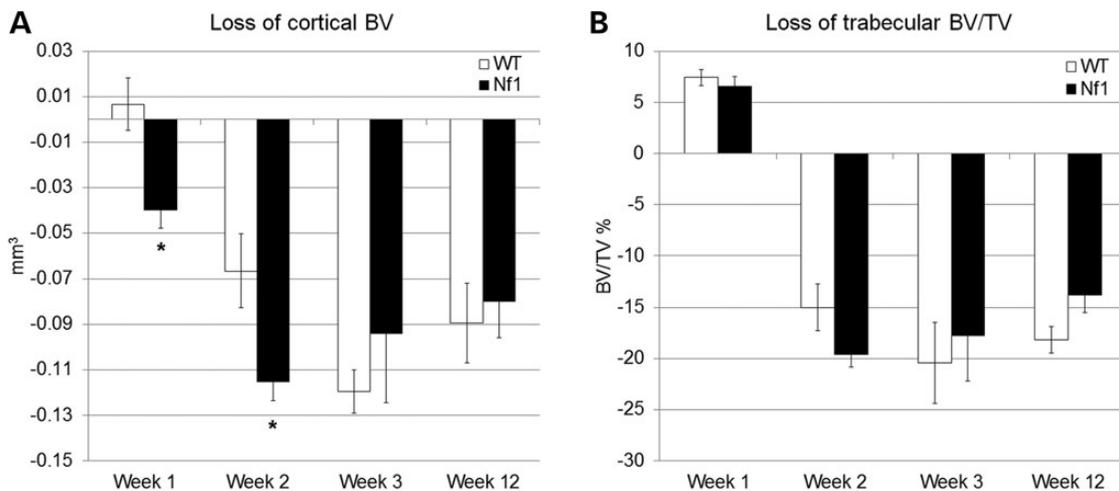

Figure 3. MicroCT analysis of the loss of diaphyseal cortical bone (BV, mm^3) and trabecular bone at the metaphysis (BV/TV, %). Bone loss was compared between WT and $Nf1^{+/-}$ genotypes. At the early time points, there was a trend towards a greater initial loss of (**A**) cortical bone in the $Nf1^{+/-}$ mice immediately following unloading (*$P < 0.05$). No differences were seen with (**B**) trabecular bone compartment.
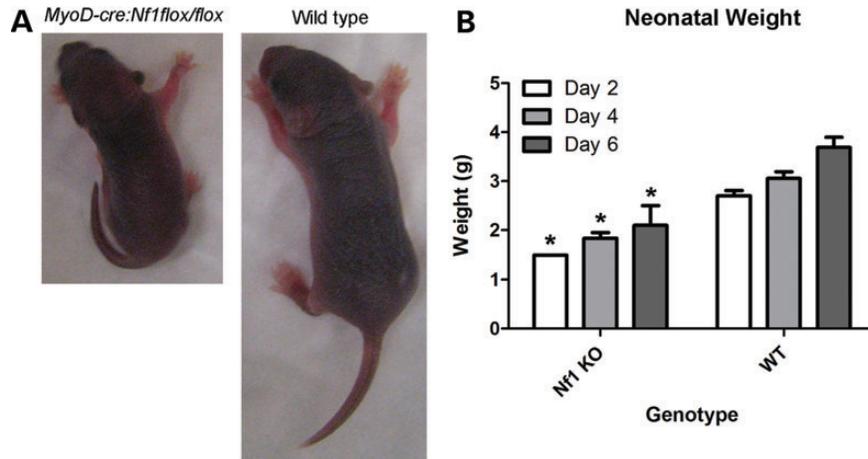
Figure 4. Reduced weight in $Nf1_{muscle}^{-/-}$ mice. In the $Nf1_{muscle}^{-/-}$ mice (*MyoD-cre:Nf1^{flox/flox}* genotype), neonatal body weight was significantly reduced at day 4 in muscle knockouts compared with WT and heterozygous littermate controls. (**A**) Representative images of knockout and WT littermate pups. (**B**) Mean weights of $Nf1_{muscle}^{-/-}$ pups and WT littermates at days 2, 4, and 6 are shown. Multi-group analysis by ANOVA showed significance based on age ($P < 0.05$) and genotype ($P < 0.05$).
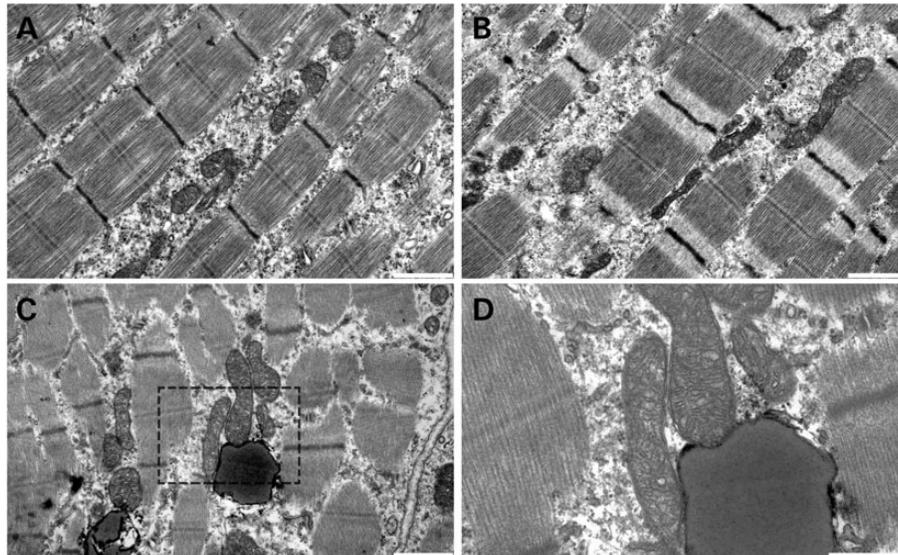

Figure 5. EM of $Nf1_{muscle}^{-/-}$ muscle. No difference in sarcomeric structure was seen between WT muscle (**A**) and $Nf1_{muscle}^{-/-}$ muscle (**B**) at day 4. Globules of what appeared to be lipid were seen in the $Nf1_{muscle}^{-/-}$ samples (**C**, inset **D**). Scale bar = 1 μm (A–C), 500 nm (D).

no abnormalities were seen in the muscle sarcomere (Fig. 5A and B). While some abnormal (large or elongated) mitochondria were noted in the $Nf1_{muscle}^{-/-}$ samples, the majority of mitochondria appeared normal and no mitochondrial breakdown was seen. Notably, intramyocellular inclusions that were speculated to contain lipid were observed in the $Nf1_{muscle}^{-/-}$ mice with a greater frequency than controls.

Altered muscle metabolism in $Nf1_{muscle}^{-/-}$ and $Nf1_{Prx1}^{-/-}$ mice

$Nf1_{muscle}^{-/-}$ mice failed to thrive and by day 6 showed significant morbidity and mortality. Tissue from day 4 pups was examined to determine any initial changes in muscle histology. No significant difference was seen in muscle fiber size at this time point ($P >$

0.05). Even at a later time point of day 6, no differences were seen by Gomori Trichrome staining, which is used to detect mitochondrial myopathy (Fig. 6A–D). Based on the lipid noted by EM, an Oil Red O stain was performed and this revealed marked accumulation of lipid droplets in the $Nf1_{muscle}^{-/-}$ mouse muscle (Fig. 6E–H, Supplementary Material, Fig. S3). These droplets varied considerably in size but were discrete droplets in the muscle tissue and not adipocytes/intermuscular fat. Quantitation showed a significant increase in the amount of intramyocellular lipid in $Nf1_{muscle}^{-/-}$ muscle ($P < 0.01$, Fig. 6I).

Non-quantitative NADH and succinate dehydrogenase (SDH) staining suggested that metabolic activity may be affected in the muscle-specific knockout mice (data not shown); therefore quantitative metabolic activity assays were performed on muscle extracts from $Nf1_{muscle}^{-/-}$ and $Nf1_{Prx1}^{-/-}$ mice. Due to
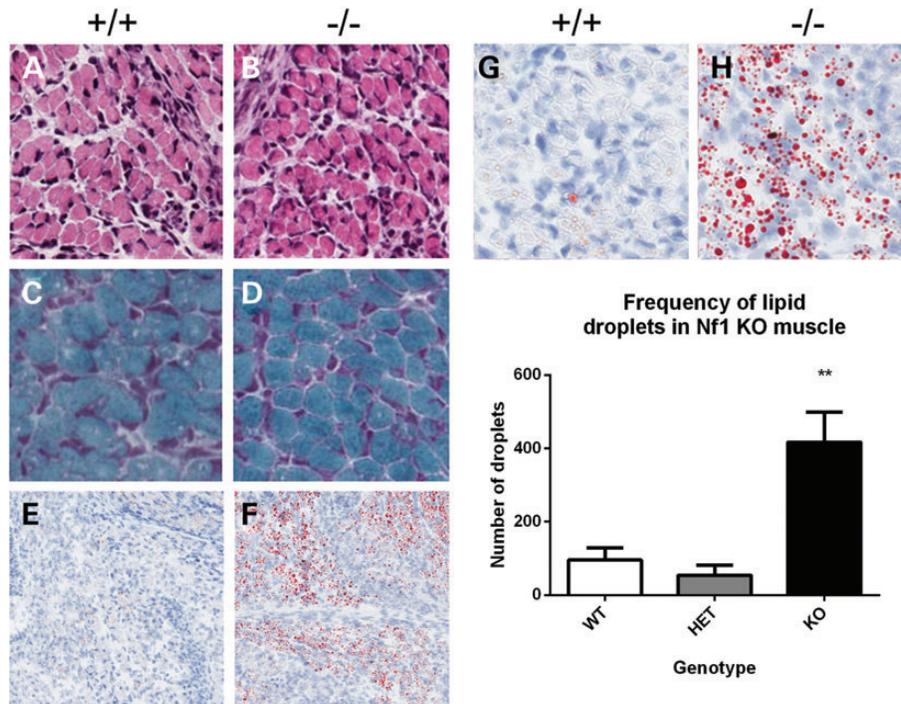
Figure 6. Muscle histology of $Nf1_{muscle}{}^{-/-}$ mice. No differences in muscle histology were seen by Haemotoxylin and Eosin staining (**A** and **B**) or Gomori Trichrome staining (**C** and **D**) between WT and $Nf1_{muscle}{}^{-/-}$ samples. Oil Red O staining revealed a dramatic increase in the frequency of lipid droplets in the muscle (**E**, **F**; zoom in **G**, **H**), which was confirmed by quantitation (**I**).

the neonatal lethality of the $Nf1_{muscle}{}^{-/-}$, whole hind limbs were collected at day 2. In addition, we obtained mature muscle tissue from $Nf1_{Prx1}{}^{-/-}$ mice. This latter strain has the *Nf1* gene knocked out in the entire limb, including the myofibers, adipocytes and vascular cells, yet the mice survive as previously reported (12). Muscle tissue was dissected from the hind limbs of 2 months $Nf1_{Prx1}{}^{-/-}$ mice. Mitochondrial enzymes SDH, citrate synthase (CS), β-hydroxyacyldehydrogenase (BHAD) and medium-chain acyl-CoA dehydrogenase (MCAD) were tested and compared with WT littermate controls. No differences were seen in the $Nf1_{muscle}{}^{-/-}$ samples, but there were 2-fold increases in SDH, BHAD and MCAD activity for the $Nf1_{Prx1}{}^{-/-}$ samples relative to littermate controls ($P < 0.05$) (Fig. 7).

Further analysis of the $Nf1_{Prx1}{}^{-/-}$ mice showed considerable increases in triglyceride content of almost 10-fold (Fig. 8A). This was consistent with observation of increased intramyocellular fat deposits in the neonatal $Nf1_{muscle}{}^{-/-}$ line. Muscle extracts from the quadriceps of $Nf1_{Prx1}{}^{-/-}$ mice and littermate controls were analyzed by western panels (Fig. 8B). No differences were seen in the expression of OXPHOS complexes, PPARγ1,2 or UCP3. Notably, however, significant increases were seen in the expression of fatty acid synthase (FAS) and leptin. We also observed decreased levels of fatty acid transport proteins carnitine palmitoyl transferase-1, CD36 and FATP4.

DISCUSSION

NF1 belongs to the RASopathy class of diseases, and the *NF1* gene product is a negative regulator of Ras GTPase activity. The RASopathies are a family of diseases that include Noonan syndrome, Costello syndrome and cardiofaciocutaneous syndrome. Since initiating our study in multiple mouse lines, the paradigm of NF1 muscle has advanced to suggest that bone and muscle involvement could be a feature of all RASopathies (22,23). To further study this concept, Stevenson and coworkers undertook studies of muscle function in jumping and grip strength tests (24,25). Their 2011 study used force plate and hand-held dynamometer testing to show that hip extension strength was decreased in NF1 patients. Nevertheless, overall jumping and hopping force production was not significantly different, potentially reflecting compensation by other muscles groups and/or insufficient statistical power. A subsequent study in 2012 measured grip strength in a range of RASopathies and found peripheral muscle weakness in all patient cohorts, including NF1 (22).

In this study, we have gone on to examine the effects of NF1 deficiency on muscle in a number of different genetically modified mouse models. Previous work with the $Nf1_{Prx1}{}^{-/-}$ mouse that lacks *Nf1* in the limb mesenchyme revealed that this can lead to muscle weakness and a dystrophy-like phenotype (12). Additional fat has also been observed in this line (26). However, this is the first study to also examine muscle in the $Nf1^{+/-}$ and $Nf1_{muscle}{}^{-/-}$ mouse lines, which show less and more severe phenotypes, respectively.

The $Nf1^{+/-}$ mouse model was generated in 1994 and has been extensively explored as a model of human disease (17). In some instances, this line adequately reflects the clinical features of NF1, such as showing impaired fracture healing that parallels orthopedic NF1 patients (20). In this study, we also show that $Nf1^{+/-}$ mice lose cortical bone more rapidly after Botox-induced immobilization, although their subsequent bone
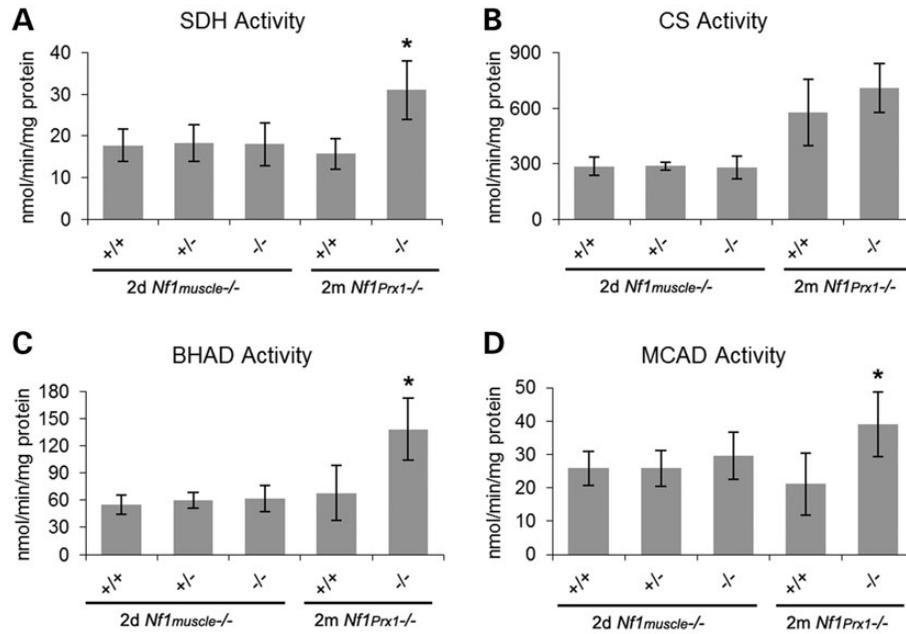
Figure 7. Mitochondrial enzyme assays for in *Nf1* knockout muscle. Enzyme assays were performed on muscle extracts from 2-day-old $Nf1_{muscle}^{-/-}$ mice and 2-month-old $Nf1_{Prx1}^{-/-}$ mice with littermate controls. SDH (**A**), CS (**B**), BHAD (**C**) and MCAD (**D**) were tested for all samples. No significant difference in metabolic enzyme activity was noted for $Nf1_{muscle}^{-/-}$ neonatal muscle for any genotype or enzyme. In contrast, mature NF1-null muscle from $Nf1_{Prx1}^{-/-}$ mice showed significant increases in SDH, BHAD and MCAD activity relative to WT controls ($P < 0.01$).

recovery is normal. This is consistent with the $Nf1^{+/-}$ line demonstrating a mild bone phenotype, although heterozygous mice fail to recapitulate many of the disease features of NF1, such as the systemic issues with bone density and bone metabolism (4,5,11). Consequentially, numerous murine models featuring double inactivation of *Nf1* have been established in order to phenocopy human manifestations not specifically associated with *NF1* double inactivation, including systemic osteopenia (27).

In this study, we found no detectable muscle phenotype in the $Nf1^{+/-}$ mice, based on histology and grip strength. While there was a trend towards a larger fiber area in 2B and 2X fibers, this did not reach statistical significance. In contrast, clinical studies have shown individuals with NF1 present with a mean decrease of at least 50% in raw handgrip strength (24). Fiber size and fiber type proportions have not been reported in individuals with NF1. In addition, immobilization-induced muscle/lean tissue loss was not different in the $Nf1^{+/-}$ mice versus controls, even though cortical bone loss was greater. Together, these data suggest that the $Nf1^{+/-}$ strain represents a poor system for modeling weakness or muscle dysfunction reported in individuals with NF1.

Subsequently, we analyzed two additional models where *Nf1* was double-inactivated either in cells of the muscle lineage using a *MyoD-cre* transgene ($Nf1_{muscle}^{-/-}$), or in the mesenchyme of the developing limb using a *Prx1-cre* transgene ($Nf1_{Prx1}^{-/-}$ mouse) (18,28). Unlike the $Nf1^{+/-}$ mice, significant phenotypic effects were seen in the tissue-specific knockouts, indicating important development functions for *Nf1* in mouse muscle. This has previously been reported in the $Nf1_{Prx1}^{-/-}$ strain with a focus on the early embryonic specification and patterning of muscle, and this report demonstrated increases in MAPK signaling (12). In

this study, we have identified a novel mechanism that suggests a regulatory role for *Nf1* in mitochondrial function in mammalian muscle.

Several lines of evidence point towards the existence of a previously unrecognized mitochondrial deregulation component of NF1 pathogenesis. First, *Nf1* has been implicated in the regulation of mitochondrial function in the *Drosophila* model (16). In this model, it has been shown that loss of *nf1* causes decreased ATP synthesis and increased reactive oxygen species (ROS) production, yielding shorter life span of the fruit fly. Conversely, *nf1* overexpression increased complex I activity and decreased ROS, but CS activity remained unchanged. In the $Nf1_{Prx1}^{-/-}$ mouse, we noted an increase in SDH activity consistent with increased mitochondrial function, but CS activity was unchanged. While the same pathways were affected as in the fly models, the direction of change was inverted (loss of *Nf1* increased rather than decreased mitochondrial activity). This difference may be attributed to differences between the species, and in muscle it has been previously reported that there is increased cAMP activation in the $Nf1_{Prx1}^{-/-}$ mouse (12), whereas the fly model showed decreased cAMP (16).

Furthermore, in *Drosophila*, the effects of *nf1* on mitochondrial function were found to be independent of Ras signaling (16). However, this may not be true for mammalian cells where Ras may have a more profound influence on mitochondrial respiration. Other RASopathies can affect cellular metabolism, for example *in vitro* expression of a mutant D61G SHP2 (which results in Noonan syndrome) decreased ATP levels and mitochondrial membrane potential and increased ROS (29). Clinically, mitochondrial dysfunction has been reported in a range of RASopathies (30,31). Intriguingly, in mouse fibroblasts expressing activated V12 H-Ras, a transient increase
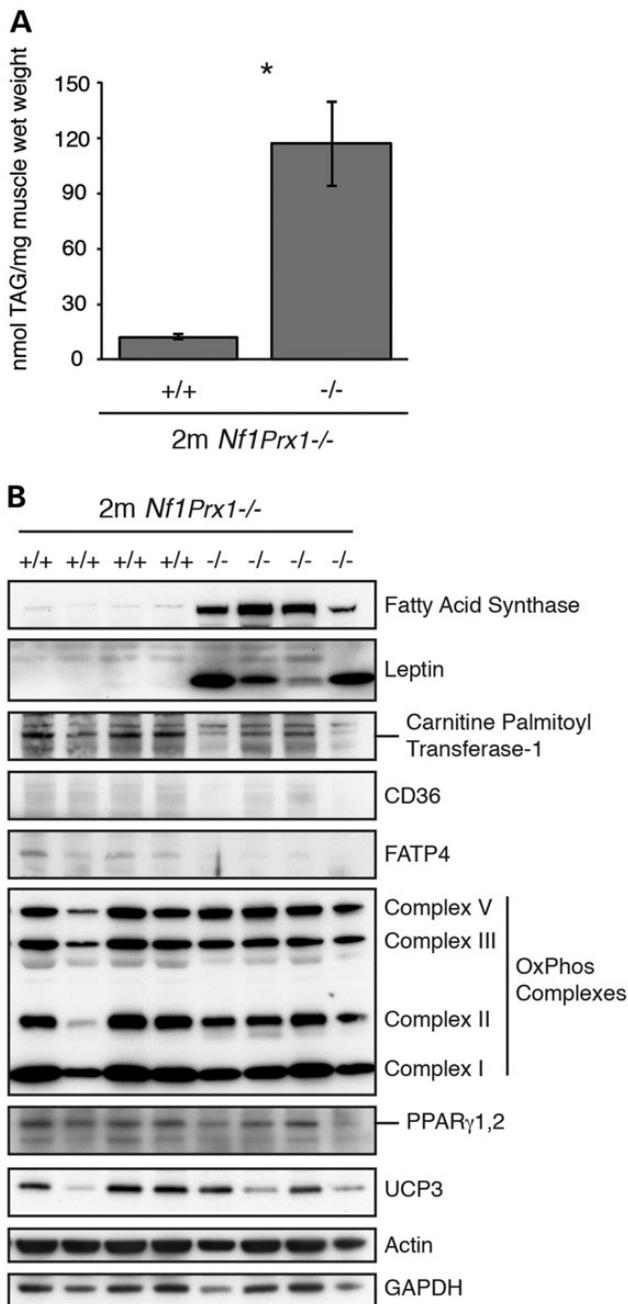
Figure 8. $Nf1_{Prx1}^{-/-}$ mice have increased muscle fat content and altered expression of fat metabolism proteins. Triglyceride content was significantly higher in $Nf1_{Prx1}^{-/-}$ mice compared with WT littermates ($n = 5$, mean $\pm$ 95% CI, $P <$ 0.01) (**A**). Western blots of quadriceps muscle extracts from $Nf1_{Prx1}^{-/-}$ mice and WT littermates ($n = 4$) equally loaded for total protein are shown (**B**). $Nf1_{Prx1}^{-/-}$ mice have higher expression of FAS and leptin and lower expression of carnitine palmitoyl transferase-1, CD36 and FATP4 compared with WT littermates, while there were no differences in expression of OxPhos complexes, PPARγ1,2 or UCP3. Actin and GAPDH are shown as loading controls.

in oxidative phosphorylation (OXPHOS) was reported to precede increased glycolysis and decreased OXPHOS (32). Thus, the molecular regulation of mitochondrial metabolism in *Nf1*-deficient muscle is likely to be complex and involve crosstalk between multiple pathways.

Notably, in neonatal muscle from the $Nf1_{muscle}^{-/-}$ line, no significant changes were seen in oxidative enzyme activity; however, the noted increase in intramyocellular lipid indicated fundamental changes in fat metabolism. Overall, the increases in SDH, BHAD and MCAD activity seen in the $Nf1_{Prx1}^{-/-}$ strain but not the $Nf1_{muscle}^{-/-}$ are likely attributable to the differences in mouse ages used and relative maturity of the tissues. However, the presence of increased metabolic activity in non-myogenic cells in the $Nf1_{Prx1}^{-/-}$ strain cannot be completely discounted and increased adipocytes have been reported in this line (26).

Further experiments will need to be undertaken to address key mechanistic and translational questions still remaining. While conditions affecting mitochondrial lipid oxidation (including deficiencies in the acyl CoA dehydrogenase family of enzymes) can lead to lipid accumulations (33), this is normally associated with impaired enzyme function, rather than increased activity as was noted in the $Nf1_{Prx1}^{-/-}$ mice. Interestingly, the $Nf1_{muscle}^{-/-}$ muscle showed lipid accumulation without mitochondrial enzyme dysfunction, potentially suggesting that the latter may develop with time as a consequence of increased lipid being present. Also consistent with this model, increases were detected in FAS, as an enzyme involved with regulating lipid biosynthesis, and leptin, a circulating hormone involved with regulating appetite and metabolism. Intriguingly, regulatory feedback may exist between neurofibromin and cellular lipid metabolism; NF1 protein stability is regulated by the ETEA/Ubxd8 ubiquitase 1, which itself is a cellular sensor of the unsaturated fatty acids (34). In addition, the observed decreases in fatty acid transport proteins could impair fat trafficking and contribute to the accumulation of intramyocellular lipids. Finally, robust experimental evidence will need to confirm whether the metabolic alterations reported in these mouse models are present in human NF1 muscle.

In conclusion, data from these mouse models support the concept that hypotonia, decreased strength and motor function in individuals with NF1 may result from abnormal Ras or cAMP signaling in the muscle, rather than being attributable purely to central nervous system dysfunction. The $Nf1^{+/-}$ model has previously been shown to not reproduce many of the clinical features of NF1 and we show that it does not replicate the muscle phenotype seen in humans. This may imply that human muscle is more dependent on Ras regulation than mouse muscle. Nevertheless, the $Nf1_{muscle}^{-/-}$ and $Nf1_{Prx1}^{-/-}$ strains show significant muscle involvement and *NF1* appears to be an important regulator of muscle metabolism.

MATERIALS AND METHODS

Mouse colonies

Animal experiments were approved by the Westmead Hospital Animal Ethics Committee or the Children's Hospital at Westmead/Children's Medical Research Institute Animal Ethics Committee. $Nf1^{+/-}$ mice were a gift from Prof Luis Parada (UT Southwestern, TX, USA) (17). $Nf1^{flox}$ mice originally generated by Prof Parada were sourced from the National Cancer Institute (NCI) mouse repository (Bethesda, MD, USA) (35). The *MyoD-Cre* mouse line expresses the Cre-recombinase gene under the control of the *MyoD* promoter (18). This mouse line

was a gift from A/Prof David Goldhamer (University of Connecticut, CN, USA). All colonies were maintained on a C57/B6 background. A PCR-based method was used to differentiate between $Nf1^{flox/flox}$ and $Nf1^{flox/+}$ genotypes and the test for the presence of the *MyoD-Cre* transgene. $Nf1_{Prx1}^{-/-}$ mice were bred in the Max Planck Institute for Molecular Genetics (Berlin, Germany) by crossing $Nf1^{flox/flox}$ and *Prx1-Cre* strains (12).

Grip strength test

A grip strength meter (Columbus Instruments) was used to test mouse forearm grip strength as recorded in Newtons (N). Mice were held by the base of the tail and allowed to grip the trapeze with their front paws and then pulled with their body parallel to the floor. Each mouse was trialed 10 times with the highest and lowest readings excluded; the remaining readings were averaged. A single experienced tester was used blinded to genotype.

Botox induced unloading

Botox injection has previously been used to injure muscle and cause unloading of the bone (36). Following this principle, WT and $Nf1^{+/-}$ mice, 48 total, aged 8 weeks were treated with Botox (1 µg) via four intramuscular injections to induce unloading of the right hind limb. Mice were analyzed by video analysis of gait until gait was considered normal, and weighed and X-rayed weekly. Weekly DEXA scans (dual X-ray absorptiometry) were also performed using a Lunar PIXImus DEXA Scanner (GE Lunar PIXImus). Time points were at 1, 2, 3 and 12 weeks. Endpoint analysis included microCT of the Botox and contra-lateral limb using a Skyscan 1174 scanner (Skyscan Corp) and isolated muscle weight measurements.

Electron microscopy

Muscle tissue was harvested from d4 post-natal pups of a *MyoD-Cre; $Nf1^{flox/+}$ × $Nf1^{flox/flox}$* cross. This generated $Nf1_{muscle}^{-/-}$, $Nf1_{muscle}^{+/-}$ and control samples. Specimens were treated with Karnovsky's fixative (R. Boadle, Institute of Clinical Pathology and Medical Research, Westmead Hospital, NSW, Australia) for 3 h at room temperature and stored in 1 × MOPS buffer. Samples were then prepared for semi-thin and ultra-thin section and examined under transmission EM.

Histological staining

Hind limb muscles were collected immediately after cull covered in cryo-preservation medium (Tissue-Tek) and frozen in partly thawed isopentane pre-chilled in liquid nitrogen. Cryosected muscle underwent trichrome stain to determine abnormalities in connective tissue or large protein accumulations. Sections were incubated in Harris Haematoxylin pH 2.3 for 5 min. Slides were then rinsed five times in distilled water and incubated in trichrome solution for 60 min [0.6% chromotype 2R (C-3143, Sigma), 0.3% Fast Green (F 7258, Sigma), 0.6% phosphotungstic acid (P 6395, Sigma), and 1% glacial acetic acid, pH 3.4]. Slides were then rinsed in 0.2% acetic acid followed by dehydration through ethanol gradients (70, 95, 100%) and mounting. Oil Red O stain was used to determine the presence of lipid accumulation in the muscle tissue. Cryosections were rinsed in 60% isopropanol before staining with Oil Red O stain solution. Stain solution is prepared from a stock solution (0.5 g Oil Red O in 100 ml isopropanol) dissolved 3:2 in dH_2O. Slides were incubated for 15 min in stain solution, before rinsing with 60% isopropanol. Slides were counterstained with hematoxylin and rinsed in water before mounting in aqueous media. Quantification was performed using BioQuant Analysis System to select red oil droplets within the section (Nashville, TN, USA).

Fiber size measurements were performed on transverse 8 µm sections from the *tibialis anterior*. Sections were stained by immunohistochemistry for fiber type using antibodies against myosin isoforms, and membrane was staining was performed using an anti-dystrophin antibody. Fiber size measurements were performed with users blinded to genotype. Cross-sectional fiber diameter was defined as the length of the longest chord perpendicular to the longest distance that stretches through the center of the fiber. Fiber diameters were measured using calibrated Image-Pro Plus 2.0 software (Media Cybernetics, Silver Spring, MD, USA). Methods for immunostaining and quantitation were performed as previously published with no modifications to the protocol (37).

Enzyme assays

Extracts were prepared from the snap frozen quadriceps muscles of 8-week-old $Nf1_{Prx1}^{-/-}$ and $Nf1_{Prx1}^{+/+}$ mice and from snap frozen skinned hind-limbs of 2-day-old Nf1 $Nf1_{muscle}^{-/-}$, $Nf1_{muscle}^{+/-}$ and $Nf1_{muscle}^{+/+}$ mice. The activities of the enzymes CS (EC 4.1.3.7) 3-hydroxyacyl-CoA dehydrogenase (BHAD, EC 1.1.1.35), medium chain acyl-CoA dehydrogenase (MCAD, EC 1.3.99.3) and succinate dehydrogenase (SDH, 1.3.5.1) were determined by spectrophotometry in muscle homogenates using methods described previously (38). Assays were performed at 30°C in duplicate and values were averaged. Activities were corrected for total protein content as measured using the BioRad Protein Assay (500-0006), according to the manufacturer's instructions, for BSA standards and extracts in duplicate. The mg protein in each extract was used to convert the activities of each enzyme (mU) to specific activities (mU/mg or nmol/min/mg protein).

Muscle triglyceride assay

Muscle triglycerides were determined in quadriceps muscles from 8-week-old $Nf1_{Prx1}^{-/-}$ and control ($Nf1_{Prx1}^{+/+}$) mice using a colorimetric assay kit (Triglycerides GPO-PAP; Roche Diagnostics, Indianapolis, IN, USA).

Western blots

Western blots were performed on quadriceps muscles from 8-week-old $Nf1_{Prx1}^{-/-}$ and $Nf1_{Prx1}^{+/+}$ mice. Samples were prepared in 4% SDS lysis buffer and total protein content was determined using a BCA assay kit (Pierce 23225) with a BSA standard curve. Eight microgram of total protein/sample was run on 4–12% Bis-Tris precast gels (Invitrogen) in MOPS buffer. Proteins were transferred to PVDF membrane. Antibodies used for western blotting were Fatty Acid Synthase (Cell Signalling

C20G5 1:1000), Carnitine Palmitoyl Transferase-1 Muscle (Alpha Diagnostics CPT1-M 1:1000), Western Blotting Detection Kit for OxPhos Complexes (Mito Science MS601 1:10000), CD36 (Santa Cruz sc-9154 1:1000), PPARγ1,2 (Biomol SA-206 1:1000), Leptin (Sigma L3410 1:1000), FATP4 (Abcam ab72721 1:1000), UCP3 (Thermo PA1-055 1:1000), Actin (Sigma 5C5 1:10000) and GAPDH (Millipore MAB374 1:10000).

Statistical analyses

Cell culture assays were conducted in triplicate at least. Values are presented as mean $\pm$ standard error (SE), and statistical comparisons were made using parametric two-tailed Student's t-tests. P-values of $P < 0.05$ were considered statistically significant.

For mouse studies, it was unclear whether data fit a normal distribution so more stringent non-parametric statistical tests were performed. Data were tested by Mann–Whitney U (two-independent groups) or a Kruskal–Wallis test (K independent groups) using SPSS Legacy Non-Parametric testing software (SBSS Statistics v19). Again, P values of $P < 0.05$ were considered statistically significant. Error bars represent the standard error of the mean.

SUPPLEMENTARY MATERIAL

Supplementary Material is available at *HMG* online.

REFERENCES

1. Friedman, J.M. (2002) Neurofibromatosis 1, clinical manifestations and diagnostic criteria. *J. Child. Neurol.*, **17**, 548–554.

2. Schindeler, A. and Little, D.G. (2008) Recent insights into bone development, homeostasis, and repair in type 1 neurofibromatosis (NF1). *Bone*, **42**, 616–622.

3. Gutmann, D.H., Aylsworth, A., Carey, J.C., Korf, B., Marks, J., Pyeritz, R.E., Rubenstein, A. and Viskochil, D. (1997) The diagnostic evaluation and multidisciplinary management of neurofibromatosis 1 and neurofibromatosis 2. *JAMA*, **278**, 51–57.

4. Kuorilehto, T., Pöyhönen, M., Bloigu, R., Heikkinen, J., Väänänen, K. and Peltonen, J. (2005) Decreased bone mineral density and content in neurofibromatosis type 1, lowest local values are located in the load-carrying parts of the body. *Osteoporos. Int.*, **16**, 928–936.

5. Lammert, M., Kappler, M., Mautner, V.F., Lammert, K., Störkel, S., Friedman, J.M. and Atkins, D. (2005) Decreased bone mineral density in patients with neurofibromatosis 1. *Osteoporos. Int.*, **16**, 1161–1166.

6. Tucker, T., Schnabel, C., Hartmann, M., Friedrich, R.E., Frieling, I., Kruse, H.P., Mautner, V.F. and Friedman, J.M. (2009) Bone health and fracture rate in individuals with neurofibromatosis 1 (NF1). *J. Med. Genet.*, **46**, 259–265.

7. Stevenson, D.A., Zhou, H., Ashrafi, S., Messiaen, L.M., Carey, J.C., D'Astous, J.L., Santora, S.D. and Viskochil, D.H. (2006) Double inactivation of NF1 in tibial pseudarthrosis. *Am. J. Hum. Genet.*, **79**, 143–148.

8. Yu, X., Chen, S., Potter, O.L., Murthy, S.M., Li, J., Pulcini, J.M., Ohashi, N., Winata, T., Everett, E.T., Ingram, D. *et al.* (2005) Neurofibromin and its inactivation of Ras are prerequisites for osteoblast functioning. *Bone*, **36**, 793–802.

9. Gutmann, D.H., Cole, J.L. and Collins, F.S. (1994) Modulation of neurofibromatosis type 1 gene expression during in vitro myoblast differentiation. *J. Neurosci. Res.*, **37**, 398–405.

10. Feldmann, R., Denecke, J., Grenzebach, M., Schuierer, G. and Weglage, J. (2003) Neurofibromatosis type 1, motor and cognitive function and T2-weighted MRI hyperintensities. *Neurology*, **61**, 1725–1728.

11. Dulai, S., Briody, J., Schindeler, A., North, K.N., Cowell, C.T. and Little, D.G. (2007) Decreased bone mineral density in neurofibromatosis type 1, results from a pediatric cohort. *J. Pediatr. Orthop.*, **27**, 472–475.

12. Kossler, N., Stricker, S., Rödelsperger, C., Robinson, P.N., Kim, J., Dietrich, C., Osswald, M., Kühnisch, J., Stevenson, D.A., Braun, T. *et al.* (2011) Neurofibromin (Nf1) is required for skeletal muscle development. *Hum. Mol. Genet.*, **20**, 2697–2709.

13. Stevenson, D.A., Moyer-Mileur, L.J., Carey, J.C., Quick, J.L., Hoff, C.J. and Viskochil, D.H. (2005) Case-control study of the muscular compartments and osseous strength in neurofibromatosis type 1 using peripheral quantitative computed tomography. *J. Musculoskelet. Neuronal. Interact.*, **5**, 145–149.

14. Souza, J.F., Passos, R.L., Guedes, A.C., Rezende, N.A. and Rodrigues, L.O. (2009) Muscular force is reduced in neurofibromatosis type 1. *J. Musculoskelet. Neuronal. Interact.*, **9**, 15–17.

15. Johnson, B.A., MacWilliams, B.A., Carey, J.C., Viskochil, D.H., D'Astous, J.L. and Stevenson, D.A. (2010) Motor proficiency in children with neurofibromatosis type 1. *Pediatr. Phys. Ther.*, **22**, 344–348.

16. Tong, J.J., Schriner, S.E., McCleary, D., Day, B.J. and Wallace, D.C. (2007) Life extension through neurofibromin mitochondrial regulation and antioxidant therapy for neurofibromatosis-1 in Drosophila melanogaster. *Nat. Genet.*, **39**, 476–485.

17. Brannan, C.I., Perkins, A.S., Vogel, K.S., Ratner, N., Nordlund, M.L., Reid, S.W., Buchberg, A.M., Jenkins, N.A., Parada, L.F. and Copeland, N.G. (1994) Targeted disruption of the neurofibromatosis type-1 gene leads to developmental abnormalities in heart and various neural crest-derived tissues. *Genes Dev.*, **8**, 1019–1029.

18. Chen, J.C., Mortimer, J., Marley, J. and Goldhamer, D.J. (2005) MyoD-cre transgenic mice, a model for conditional mutagenesis and lineage tracing of skeletal muscle. *Genesis*, **41**, 116–121.

19. Bajenaru, M.L., Zhu, Y., Hedrick, N.M., Donahoe, J., Parada, L.F. and Gutmann, D.H. (2002) Astrocyte-specific inactivation of the neurofibromatosis 1 gene (NF1) is insufficient for astrocytoma formation. *Mol. Cell. Biol.*, **22**, 5100–5113.

20. Schindeler, A., Morse, A., Harry, L., Godfrey, C., Mikulec, K., McDonald, M., Gasser, J.A. and Little, D.G. (2008) Models of tibial fracture healing in normal and Nf1-deficient mice. *J. Orthop. Res.*, **26**, 1053–1060.

21. El-Hoss, J., Sullivan, K., Cheng, T., Yu, N.Y., Bobyn, J.D., Peacock, L., Mikulec, K., Baldock, P., Alexander, I.E., Schindeler, A. *et al.* (2012) A murine model of neurofibromatosis type 1 tibial pseudarthrosis featuring proliferative fibrous tissue and osteoclast-like cells. *J. Bone. Miner. Res.*, **27**, 68–78.

22. Stevenson, D.A. and Yang, F.C. (2011) The musculoskeletal phenotype of the RASopathies. *Am. J. Med. Genet. C Semin. Med. Genet.*, **157**, 90–103.

23. Tidyman, W.E., Lee, H.S. and Rauen, K.A. (2011) Skeletal muscle pathology in Costello and cardio-facio-cutaneous syndromes, developmental consequences of germline Ras/MAPK activation on myogenesis. *Am. J. Med. Genet. C Semin. Med. Genet.*, **157**, 104–114.

24. Johnson, B.A., Macwilliams, B., Carey, J.C., Viskochil, D.H., D'Astous, J.L. and Stevenson, D.A. (2012) Lower extremity strength and hopping and jumping ground reaction forces in children with neurofibromatosis type 1. *Hum. Mov. Sci.*, **31**, 247–254.

25. Stevenson, D.A., Allen, S., Tidyman, W.E., Carey, J.C., Viskochil, D.H., Stevens, A., Hanson, H., Sheng, X., Thompson, B.A., Okumura, M.J. *et al.* (2012) Peripheral muscle weakness in RASopathies. *Muscle Nerve*, **46**, 394–399.

26. El Khassawna, T., Toben, D., Kolanczyk, M., Schmidt-Bleek, K., Koennecke, I., Schell, H., Mundlos, S. and Duda, G.N. (2012) Deterioration of fracture healing in the mouse model of NF1 long bone dysplasia. *Bone*, **51**, 651–660.

27. Rhodes, S.D., Wu, X., He, Y., Chen, S., Yang, H., Staser, K.W., Wang, J., Zhang, P., Jiang, C., Yokota, H. *et al.* (2013) Hyperactive transforming growth factor-β1 signaling potentiates skeletal defects in a neurofibromatosis type 1 mouse model. *J. Bone. Miner. Res.*, [23 May, Epub ahead of print].

28. Logan, M., Martin, J.F., Nagy, A., Lobe, C., Olson, E.N. and Tabin, C.J. (2002) Expression of Cre Recombinase in the developing mouse limb bud driven by a Prxl enhancer. *Genesis*, **33**, 77–80.

29. Lee, I., Pecinova, A., Pecina, P., Neel, B.G., Araki, T., Kucherlapati, R., Roberts, A.E. and Hüttemann, M. (2010) A suggested role for mitochondria in Noonan syndrome. *Biochim. Biophys. Acta*, **1802**, 275–283.

30. Kleefstra, T., Wortmann, S.B., Rodenburg, R.J., Bongers, E.M., Hadzsiev, K., Noordam, C., van den Heuvel, L.P., Nillesen, W.M., Hollody, K., Gillessen-Kaesbach, G. *et al.* (2011) Mitochondrial dysfunction and organic aciduria in five patients carrying mutations in the Ras-MAPK pathway. *Eur. J. Hum. Genet.*, **19**, 138–144.

31. Aeby, A., Sznajer, Y., Cavé, H., Rebuffat, E., Van Coster, R., Rigal, O. and Van Bogaert, P. (2007) Cardiofaciocutaneous (CFC) syndrome associated with muscular coenzyme Q10 deficiency. *J. Inherit. Metab. Dis.*, **30**, 827.

32. de Groof, A.J., te Lindert, M.M., van Dommelen, M.M., Wu, M., Willemse, M., Smift, A.L., Winer, M., Oerlemans, F., Pluk, H., Fransen, J.A. *et al.* (2009) Increased OXPHOS activity precedes rise in glycolytic rate in H-RasV12/E1A transformed fibroblasts that develop a Warburg phenotype. *Mol. Cancer*, **8**, 54.

33. Laforêt, P. and Vianey-Saban, C. (2010) Disorders of muscle lipid metabolism, diagnostic and therapeutic challenges. *Neuromuscul. Disord.*, **20**, 693–700.

34. Phan, V.T., Ding, V.W., Li, F., Chalkley, R.J., Burlingame, A. and McCormick, F. (2010) The RasGAP proteins Ira2 and neurofibromin are negatively regulated by Gpb1 in yeast and ETEA in humans. *Mol. Cell. Biol.*, **30**, 2264–2279.

35. Zhu, Y., Ghosh, P., Charnay, P., Burns, D.K. and Parada, L.F. (2002) Neurofibromas in NF1, Schwann cell origin and role of tumor environment. *Science*, **296**, 920–922.

36. Warner, S.E., Sanford, D.A., Becker, B.A., Bain, S.D., Srinivasan, S. and Gross, T.S. (2006) Botox induced muscle paralysis rapidly degrades bone. *Bone*, **38**, 257–264.

37. Garton, F., Seto, J.T., North, K.N. and Yang, N. (2010) Validation of an automated computational method for skeletal muscle fibre morphometry. *Neuromusc. Disord.*, **20**, 540–547.

38. MacArthur, D.G., Seto, J.T., Chan, S., Quinlan, K.G., Raftery, J.M., Turner, N., Nicholson, M.D., Kee, A.J., Hardeman, E.C., Gunning, P.W. *et al.* (2008) An Actn3 knockout mouse provides mechanistic insights into the association between α actinin-3 deficiency and human athletic performance. *Hum. Mol. Genet.*, **17**, 1076–1086.